Chapter 6

Research Article 2: Synthesis and Evaluation of Fluorescent Heterocyclic Aminoadamantanes as Multifunctional Neuroprotective Agents

Article published online on 24 May 2011

Bioorganic and Medicinal Chemistry 19 (2011) 3935-3944

Synthesis and Evaluation of Fluorescent Heterocyclic Aminoadamantanes as Multifunctional Neuroprotective Agents

Jacques Joubert[a,b] Sandra v Dyk[a] Ivan R. Green[c] and Sarel F. Malan[a,b,*]

[a]*Pharmaceutical Chemistry, North-West University, Private Bag 6001, Potchefstroom, 2520 , South Africa.* [b]*School of Pharmacy and* [c]*Department of Chemistry, University of the Western Cape, Bellville, South Africa, Private Bag X17, Bellville 7535, South Africa.*

*Corresponding author at present address: School of Pharmacy, University of the Western Cape, Private Bag X17, Bellville 7535, South Africa. Tel: +27 21959 3190; fax: +27 21959 1588; e-mail: sfmalan@uwc.ac.za

Graphical abstract

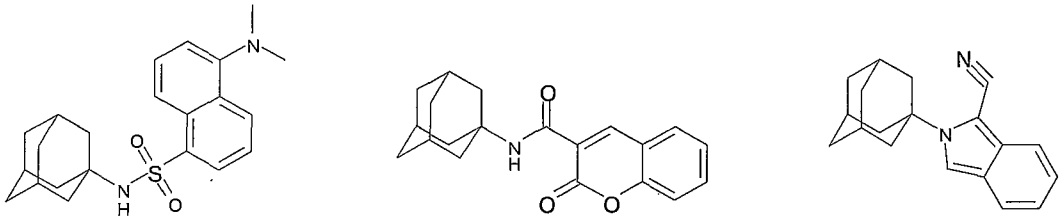

A series of fluorescent heterocyclic adamantine derivatives were found to possess a high degree of multifunctional neuroprotective activity.

Abstract

A series of fluorescent heterocyclic adamantane amines were synthesised with the goal to develop novel fluorescent ligands for neurological assay development. These derivatives demonstrated multifunctional neuroprotective activity through inhibition of the *N*-methyl-D-aspartate receptor/ion channel, calcium channels and the enzyme nitric oxide synthase. It also exhibited a high degree of free radical scavenging potential. *N*-(1-adamantyl)-2-oxo-chromene-3-carboxamide (**8**), *N*-adamantan-1-yl-5-dimethyl-amino-1-naphthalenesulfonic acid (**11**) and *N*-(1-cyano-2*H*-isoindol-2-yl)adamantan-1-amine (**12**) were found to possess a high degree of multifunctionality with favourable physical-chemical properties for bioavailability and blood-brain barrier permeability. The ability of these heterocyclic adamantane amine derivatives as nitric oxide synthase inhibitors, calcium channel modulators, NMDAR inhibitors and effective antioxidants, indicate that they may find application as multifunctional drugs in neuroprotection.

Keywords: Amantadine, NMDA Receptor, Antioxidant Activity, Neuroprotection, Calcium Channels, NOS Inhibition

6.1. Introduction

Progressive neurodegenerative disorders such as Parkinson's, Alzheimer's and Huntington's disease as well as acute conditions like stroke greatly reduce the quality of life of patients suffering from these conditions and is becoming a burden to society as the world's population becomes older.[1] Currently there are relatively good symptomatic treatment for neurodegenerative disorders. However, no proven therapy that prevents cell death nor restores damaged neurons to a normal state has as yet been developed.[2] Several drug targets have been identified that would act either as a symptomatic and/or neuroprotective treatment for neurodegenerative disorders. These include, amongst others, inhibitors/antagonists of the dopamine transporter (specifically for Parkinson's Disease), voltage dependant calcium channels (VDCC), *N*-methly-D-aspartate receptors (NMDAR), neuronal nitric oxide synthase (nNOS), and detrimental reactive oxygen/nitrogen free radicals derived from oxidative stress. These form part of the three main mechanisms of neuronal cell death that may act separately or cooperatively to cause neurodegeneration,[3] namely excitotoxicity, oxidative stress and metabolic compromise that is both necrotic and apoptotic in nature.

Excitotoxicity is a pathological process in which neuronal death occurs due to the over stimulation of NMDAR, an event that causes an excessive influx of calcium ions into neuronal cells.[4] In addition, calcium entering through the VDCC is implicated in calcium overload and mitochondrial disruption.[5,8] Calcium overloading can cause the activation of calcium-dependant signals to enzymes, such as phospholipases and proteases, as well as oxidative stress through reactive oxygen species (ROS) and reactive nitrogen species (RNS).[5,6,7] Dysfunction of the mitochondria leads to a loss of intracellular calcium buffering capacity and an increase in the production of damaging ROS and RNS, leading to oxidative stress.[5,7] Oxidative stress is caused by the actions of highly reactive oxygen species such as superoxide anions (O_2^-), hydroxyl radicals ($^{\cdot}OH$) and reactive nitrogen species such as peroxynitrite ($ONOO^-$). The oxidizing actions of these reactive species destroy membrane lipids, proteins and DNA and could thus cause neurodegeneration at excessive concentrations. Production of free radicals can be enhanced by various substances including intracellular calcium, dopamine and nitric oxide synthase (NOS).[5,7] Calcium overload also stimulates the production of the calcium dependant neuronal nitric oxide synthase (nNOS), an enzyme that catalyses the formation of nitric oxide (NO) in the central nervous system (CNS). Overstimulation of nNOS and subsequent overproduction of NO is known to lead to the development of neurodegenerative processes and cell death.[9] Harmful effects caused by an overproduction of NO are thought to be mediated by peroxynitrate ($ONOO^-$), the product obtained when NO and the superoxide anion (O_2^-) react. Peroxnitritrate ($ONOO^-$) causes injury to the mitochondrial electron transport chain resulting in damage and eventual neurodegeneration and death of neurons.[9,10]

From the above discussion it is clear that neurodegenerative disorders are complex diseases with multiple pathways which contribute to their etiology and finally cell death of CNS neurons.[11] A drug with a single-target mechanism of action cannot always compensate for, or correct these complex pathways. Polypharmaceutical approaches have been applied as a means of multiple targeting in a clinical setting, wherein several drugs act independently on various biological targets of the disease. However this strategy has several drawbacks, such as multiple toxicities and side-effects of the individual drugs. Additionally the occurrence of unexpected drug-drug interactions and other conditions may occur.[12] For these reasons, one drug molecule that possess promiscuous activity acting on more than one biological target in the cell death cascades has to be investigated or designed. The advantages associated with this strategy includes a lower likelihood of encountering unwanted side-effects and the possibility

to increase therapeutic index by simple structural modifications.[13] Current polycyclic derivatives with adamantane and pentacycloundecane scaffolds described in literature as multifunctional neuroprotective agents include, amantadine (**1**), memantine (**2**), NGP1-01 (**3**), M30K (**4**), M30L (**5**) and compound **6** (Figure 1). Amantadine (**1**) expresses multimodal neuroprotective activity through the increment of extracellular dopamine levels *via* dopamine re-uptake inhibition[14] and dopamine release, which may be additionally useful in treatment of the motor symptoms of Parkinson's disease, as well as NMDAR antagonism.[15] Memantine (**2**) may further possess a dual mechanism by direct blockade of the NMDAR and by attenuating tumour necrosis factor alpha (TNFα)-induced potentiation of glutamate toxicity.[16,17] NGP1-01 is a dual-mechanism drug which blocks both the NMDAR as well as the *L*-type calcium channels and may also inhibit dopamine reuptake, with resulting neuroprotective activity shown *in vivo*.[17-23] M30K and M30L are multimodal free radical scavengers, MAO-B and cholinesterase inhibitors.[24] Compound **6** has been developed by Neuraxon as a dual NMDA receptor/ion channel- and selective nNOS inhibitor for multifunctional neuroprotection.[25] These drugs may have the advantage of acting at several sites in the brain and be of particular value in neuroprotective stratergies.[26,27]

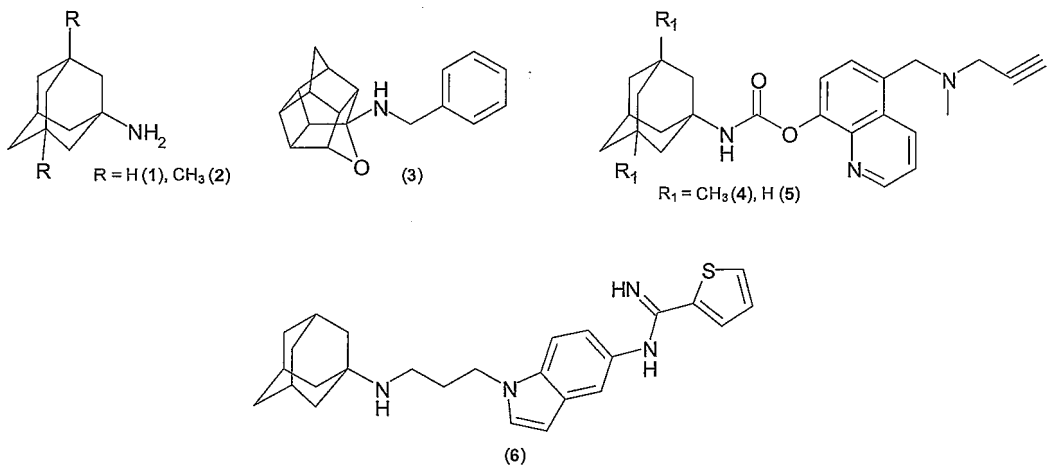

Figure 1: Multifunctional polycyclic neuroprotective agents previously described.

In the search to improve our knowledge on neurodegenerative mechanisms we set out to develop fluorescent adamantane amine derivatives as ligands in the development of neurological assays, amongst others, to circumvent the expensive use of radioligand binding studies.[28] Our findings in this study further prompted our interest on these molecules as potential multifunctional neuroprotective agents. We based our hypothesis on the fact that amantadine produces neuroprotective activity through increased dopamine transmission and NMDAR inhibitory activity.[14,15] It has also demonstrated the ability to stabilize the closed-

state of calcium channels during excessive influx of calcium ions. The choice of amantadine was further justified by the fact that its NMDAR blockage is use-dependent and it modulates, rather than blocks calcium channels.[1] This will ensure that normal calcium influx and NMDA receptor functions are maintained. Amantadine was also shown to increase the blood brain barrier (BBB) permeability of privileged moieties conjugated to it, which is desirable for greater CNS drug effect.[29] Furthermore in a previous study done in our laboratories,[28] fluorescent ligands structurally related to 7-nitroindazole (7-NI; a potent selective nNOS inhibitor),[30,31] were conjugated to amantadine and were found to have moderate to potent NOS inhibitory activity. Fluorescent ligands structurally similar to 7-NI were developed using different bioisosteric substitutions while maintaining certain pharmacophoric groups.

In continuation of our research, we hypothesized that the conjugation of amantadine to these fluorescent heterocyclic moieties would result in novel compounds that might exhibit activity as multifunctional neuroprotective agents through inhibition of NMDAR, VDCC and NOS. Additionally these molecules could have the structural requirements to scavenge free radicals, increase dopamine transmission in the CNS and cross the BBB in high concentrations. Compounds that inhibit NMDAR, VDCC, NOS and scavenge free radicals may find enhanced application in the treatment of neurodegenerative disorders through their multifunctional mechanism of action. Since these compounds are considered for oral delivery with a high degree of BBB permeability, they were also subjected to Lipinski's rule of five.[32] Finally, the toxicity of the compounds was evaluated using the online Orisis property explorer to determine their potential as safe lead compounds.

6.2. Results

6.2.1. Synthesis

The target fluorescent heterocyclic adamantane amine derivatives were synthesised through conjugation of the fluorescent heterocyclic moieties to the amantadine moiety by amidation and amination (Scheme 1). The fluorescent compounds synthesised include *N*-methylanthranilic acid, indazole-3-carboxylic acid, 1-fluoro-2,4-dinitrobenzene (FDB), 1-cyanoisoindole, coumarin-3-carboxylic acid and dansyl chloride (DAN) conjugated to amantadine. The anthranilic indazole and coumarin complexes were obtained through the intermediate complexes with *N,N*-carbonyldiimidazole (CDI) and yielded the amides (**7**, **8**, **9**) on reaction with the primary amine. The dinitrobenzene and dansyl complexes (**10**, **11**) were obtained through amination with the primary amine of amantadine. The fluorescent isoindole (**12**) was obtained by reaction of between *o*-phthaldialdehyde (OPD) and amantadine in the

presence of sodium cyanide. The products were all purified using conventional laboratory techniques and were obtained as oils, amorphous solids or were crystallized from organic solvents and found to be of high purity as confirmed by their ^{1}H NMR, ^{13}C NMR and high resolution MS.

6.2.2. Calcium flux inhibition

The fluorescent ratiometric indicator, Mag-Fura-2/AM, and a Cary Eclipse® fluorescence spectrometer were used to evaluate the influence of the test compounds on KCl mediated calcium influx *via* VDCC and NMDA/Glycine mediated calcium influx *via* the NMDAR in murine synaptoneurosomes. All novel fluorescent compounds and controls were tested at 100 μM. These experiments identified compounds able to inhibit VDCC and/or NMDAR calcium-influx. The results are depicted in Table 1.

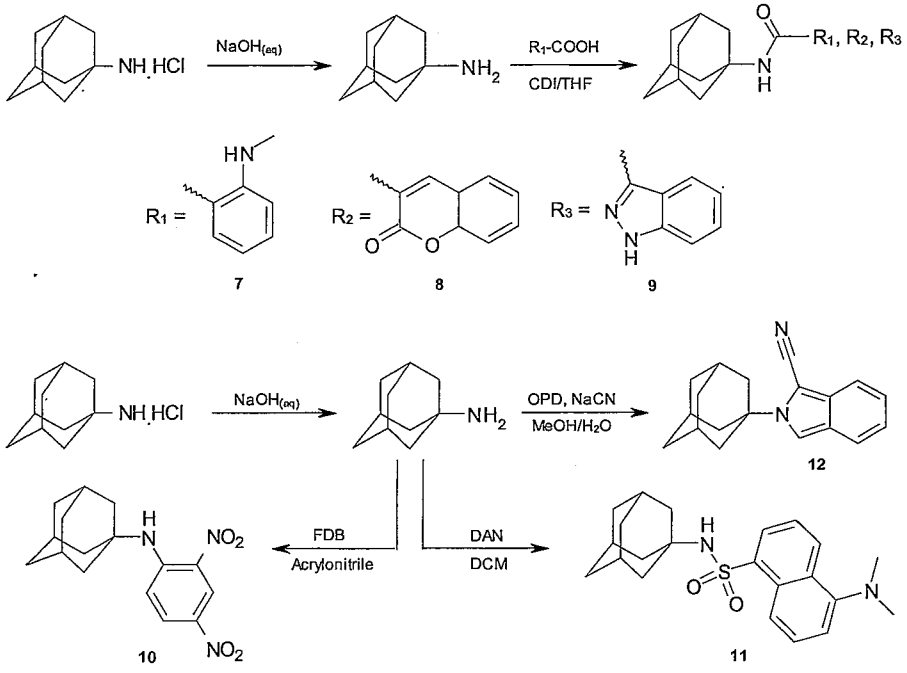

Scheme 1: General reaction scheme for the synthesis of amide (**7**, **8**, **9**) and amine (**10**, **11**, **12**) conjugates.

6.2.2.1. VDCC calcium flux inhibition

The calcium channel activities of the fluorescent heterocyclic adamantine amines were evaluated using fluorescent techniques to measure calcium flux into synaptoneurosomes. Fresh synaptoneurosomes were prepared[33] from rat brain homogenate and incubated with the ratiometric fluorescent calcium indicator, Fura-2/AM.[34] The synthesised compounds were incubated for 5 minutes and a 100 mM KCl solution was added to depolarise the cell membranes and to allow calcium to enter. Calcium influx into the cells was then monitored

based on the fluorescence intensity relative to that of a 100 % control. Three positive controls were also included: nimodipine, a commercially available dihydropyridine *L*-type calcium channel blocker, amantadine and NGP1-01 (**3**) the pentacycloundecane compound structurally related to amantadine (**1**). From the calcium flux data it was clear that nimodipine showed very high inhibition of calcium influx into the synaptoneurosomes at a concentration of 100 μM (87.71%). The results (Table 1) indicated that at the same concentration compounds **12** (45.76%) and **11** (55.23%) exhibited better calcium channel antagonism than NGP1-01 (**3**; 29.88%) and amantadine (**1**; 13.38%), with compound **8** (24.65%) exhibiting significant activity ($p < 0.05$) when compared to amantadine. Compounds **7**, **9** and **10** had weak calcium flux inhibition of between 6.57% - 11%. None of the synthesised compounds had activity comparable to nimodipine (87.71%).

6.2.2.2. NMDAR calcium flux inhibition

To evaluate the NMDAR channel modulating activity of the compounds, freshly prepared synaptoneurosomes[33] were incubated with the ratiometric fluorescent calcium indicator, Fura-2/AM.[34] The synthesised compounds were added and the cell membranes depolarised with a 100 μM NMDA/Glycine solution. Calcium influx into the cells was then monitored based on the fluorescence intensity relative to that of a 100% control. Nimodipine 10 μM was added to all preparations to reduce the possibility of calcium flux through the VDCC and to ensure selectivity for the NMDAR. Three positive controls were also included: MK-801, a commercially available potent high affinity NMDAR channel blocker, amantadine (**1**) and NGP1-01 (**3**). The results (Table 1) indicated that at a concentration of 100 μM, compounds **9** (17%), **10** (19.25%), **8** (20.29%) and **11** (21.95%) showed statistically significant ($p < 0.05$) blockage of the NMDAR and attenuated calcium flux into the cells better than the references NGP1-01 (**3**; 13.37%) and amantadine (**1**; 16.90%). Compound **12** (16%) showed lower activity than amantadine but the inhibition was statistically significant ($p < 0.05$). Compound **7** had very low inhibition of calcium flux (3.34%). None of the compounds showed activity comparable to that of MK-801 (49.4%).

From the calcium flux experiments it can be deduced that the activity of amantadine was retained or improved with the conjugation thereof to the heterocyclic moieties. It is therefore postulated that the active inhibitors contained the structural requirements for NMDAR and VDCC inhibition and could be useful in the development of new lead compounds for neurodegenerative disorders.

6.2.3. NOS inhibition

The oxyhemoglobin (oxyHb) assay[35] was employed to determine the activity of the test compounds at an enzymatic level of NOS. Rat brain homogenate was used as NOS enzyme source since it has been shown to have high constitutive nNOS activity.[36] A disadvantage of using brain homogenates as enzyme source is that isoform selectivity is unaccounted for since the crude rat brain extracts may contain smaller quantities of the other NOS isoforms. For the purpose of screening potential NOS inhibitors for CNS NOS inhibition activity, this enzyme source was deemed appropriate. The assay is principally based on the reaction of NO with oxyHb and the formation of methemoglobin (metHb). In order to determine the amount of NO formed, the change in absorbance difference between 401 and 421 nm in the UV spectra was measured during the initial linear phase of the reaction (Figure 2). With the change in absorbance at 401 nm plotted against time and the change in absorbance over time at 421 nm subtracted, the slope of the resulting curve represented an increase in the molar amount of metHb which is identical to the molar amount of NO generated. From this inhibition data the IC_{50} values were calculated and compared (Table 1).

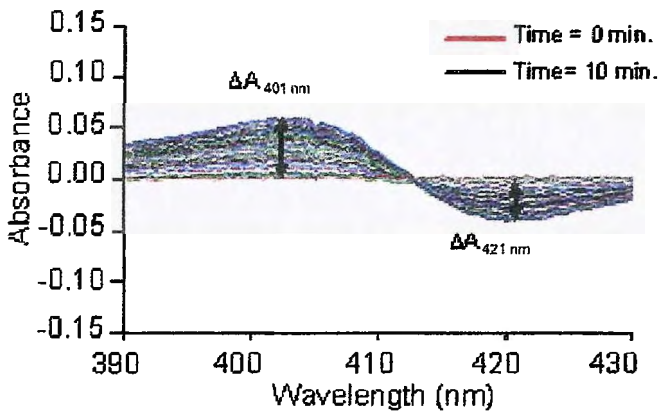

Figure 2: Spectrophotometric recording of compound **12** at a 1 μM test concentration. Continuous scans between 390 nm and 430 nm were performed as the oxyHb was converted to metHb.

inhibition of the free radicals at 3 concentrations (0.01 mM, 0.1 mM and 1 mM). The inhibition was dose dependant for all of the derivatives. Activity is expressed as the average of 9 experiments per concentration ± SEM (Table 2).

Table 2: Inhibition data for $DPPH^{\cdot+}$ and $ABTS^{+}$ assays.

Compound	%$DPPH^{\cdot+}$ ± SEM (mM)*			%$ABTS^{+}$ ± SEM (mM)*		
	0.01	0.1	1	0.01	0.1	1
7	42.74 ± 0.29	42.79 ± 0.29	44.00 ± 0.28	10.74 ± 3.42	24.29 ± 1.06	50.54 ± 1.56
8	31.77 ± 0.32	69.84 ± 0.31	91.68 ± 0.30	87.51 ± 3.43	91.79 ± 1.22	93.33 ± 2.91
9	28.71 ± 0.40	30.10 ± 0.38	32.93 ± 0.36	12.39 ± 1.34	21.72 ± 6.88	39.89 ± 5.36
10	32.14 ± 0.27	36.78 ± 0.27	37.00 ± 0.26	8.21 ± 6.58	9.73 ± 1.63	15.72 ± 1.19
11	38.02 ± 0.38	38.14 ± 0.34	40.94 ± 0.33	8.11 ± 6.85	22.45 ± 1.02	41.64 ± 5.14
12	27.41 ± 0.55	27.81 ± 0.47	32.67 ± 0.43	9.98 ± 5.14	13.22 ± 1.19	13.53 ± 3.43
Trolox	45.80 ± 0.98	74.57 ± 1.32	95.14 ± 2.43	47.60 ± 8.56	62.76 ± 5.14	88.47 ± 8.57
Amantadine	0.55 ± 0.22	2.11 ± 0.29	2.32 ± 0.38	0.49 ± 4.23	1.34 ± 6.24	1.62 ± 3.99
NGP1-01	0.20 ± 0.23	5.99 ± 0.25	9.98 ± 0.86	2.44 ± 2.11	7.33 ± 5.13	8.88 ± 3.58

*All data was found to be statistically significant ($p < 0.05$)

6.2.4.1. DPPH radical scavenging activity

Free radical scavenging activity was measured in terms of % antioxidant activity as represented in Table 2. The compounds (**7** – **12**) showed inhibition of 27.41% – 91.68%. Trolox®, used as a standard, has concentration dependant values ranging from 45.80% – 95.14%. Amantadine (0.55% - 2.32%) and NGP1-01 (0.20% - 9.98%) exhibited very low $DPPH^{\cdot+}$ radical scavenging activity. The antioxidant activity of the synthesised compounds is related to their electron or hydrogen radical releasing ability to $DPPH^{\cdot+}$ so that it becomes a stable diamagnetic molecule. The average percentage $DPPH^{\cdot+}$ radical scavenging abilities of all the adamantine heterocyclic derivatives (**7** - **12**) were lower than of Trolox®, but it was evident that these derivatives showed high reducing ability (possibly by hydrogen atom transfer) and could serve as free-radical scavengers. Compound **8** showed the most promising activity inhibiting the radical to 91.68%. Compound **12** had the lowest activity but was statistically ($p < 0.05$) active as a free radical scavenger, inhibiting $DPPH^{\cdot+}$ by 27.40% - 32.67%. This indicated that these derivatives have potential as free radical scavengers and antioxidant activity at concentrations as low as 0.01 mM.

6.2.4.2. $ABTS^{+}$ radical scavenging activity

From the $ABTS^{+}$ inhibition data (Table 3), compounds 7, **9** – **12** showed moderate to low inhibition of the $ABTS^{+}$ free radical (8.11% - 50.54%) relative to Trolox® (47.60% - 88.47%)

Table 1: Calcium flux and NOS inhibition by test compounds.

Compound	% Calcium flux (100 μM)		NOS inhibition IC_{50} (μM)
	VGCC	NMDAR	
7	93.20*	96.66	11.10*[a]
8	75.35*	79.71*	0.85*
9	93.43*	83.00*	0.35*[a]
10	89.14*	80.75*	n.a.
11	44.77*	78.05*	0.41*
12	54.24*	84.01*	0.29*[a]
Nimodipine	12.29*	n.d	n.d.
Amantadine	86.13*	83.10*	n.a.
MK-801	n.d.	64.04*	n.d.
NGP1-01	70.12*	86.63*	n.a.
7-Nitroindazole	n.d.	n.d.	0.11*
Aminoguanidine	n.d.	n.d.	19.41*

*$p < 0.05$
[a]Data taken from Joubert *et al.*[28]
n.a. = no activity
n.d. = not determined

Comparison of the IC_{50} values obtained for the heterocyclic adamantine amines to those of two known NOS inhibitors, 7-nitroindazole (7-NI; IC_{50} = 0.11 μM) and aminoguanidine (AG; IC_{50} = 19.41 μM), revealed that compounds **9**, **8**, **11** and **12** held promise as NOS inhibitors (Table 1) although none comparable to 7-NI (IC_{50} = 0.11 μM). The novel inhibitors showed significant NOS inhibition, with an IC_{50} of less than 1 μM (Table 1). Most of the compounds showed higher inhibitory activity than aminoguanidine (IC_{50} = 19.41 μM). Compound **10** as well as the multimodal polycyclic derivatives NGP1-01, (**3**) and amantadine (**1**) exhibed no inhibition of NOS. The increased activity of the compounds conjugated to amantadine could be attributed to the high degree of lipophilicity and membrane permeability and structural similarities to 7-NI. Additional assays need to be conducted on the active derivatives to determine their selectivity for the neuronal NOS isoform.

6.2.4. Antioxidant activity

Reactive oxygen and nitrogen species contribute to the pathophysiology of neurodegenerative disorders.[37] Antioxidants are compounds capable of scavenging free radicals and thus antioxidant therapy is therefore considered as one of the options in neuroprotection.[38] Antioxidant activities of the amantadine heterocycles were determined as an index of pharmacological usefulness. Two assays were used viz., the $DPPH^{\cdot+}$ and $ABTS^{+}$ radical scavenging assays. The synthetic nitrogen-centred $DPPH^{\cdot+}$ and $ABTS^{+}$ radicals are not biologically relevant, but are used as indicator compounds in testing hydrogen transfer capacity related to antioxidant activity.[39] Antioxidant properties are expressed as percentage

with the exception of compound **8** (87.51% - 93.33%). Compounds **7**, **9** and **11** showed moderate inhibition, but at higher concentration (1 mM) these derivatives have relatively high activity between 40% – 51%. The inhibition of **10** and **12** was low (< 15%) while that of amantadine (**1**; 0.49% - 1.62%) and NGP1-01 (**3**; 2.44% - 8.88%) were negligible. This indicated that compounds **7**, **9**, **11** and especially **8** had the electron or hydrogen radical releasing ability to scavenge free radicals and show potential as antioxidants.

6.3. Discussion

The current study has identified heterocyclic fluorescent adamantine amine derivatives as promising novel multifunctional neuroprotective agents that may serve as clinically useful molecules, or may lead to the development of new compounds for treatment of neurodegenerative disorders with multifunctional neuroprotective activity. The derivatives showed favourable activities for multiple neuroprotective biological functions (Table 3). Compounds to be highlighted are *N*-(1-adamantyl)-2-oxo-chromene-3-carboxamide (**8**) and *N*-adamantan-1-yl-5-dimethyl-amino-1-naphthalenesulfonic acid (**11**). Both derivatives showed a high degree of multifunctional activity in the systems tested (Table 3). Compound **8** showed highly potent antioxidant activity, comparable to and even higher than of Trolox®. It also showed potent NOS inhibition and moderate calcium channel as well as NMDAR inhibitory activity against the relevant standards. Compound **11** had potent NOS inhibition with moderate antioxidant activity and calcium modulating properties. The dansyl and coumarin heterocyclic moieties have been described throughout literature as privileged structures and the results obtained indicated that further studies need to be conducted on these derivatives to evaluate their true potential. Additionally, *N*-adamantan-1-yl-1*H*-indazole-3-carboxamide (**9**) and *N*-(1-cyano-2*H*-isoindol-2-yl) adaman-tan-1-amine **(12)** also showed favorable multifunctional activity but to a lower degree than **8** and **11**. Compound **9** was found to be a potent NOS inhibitor with a low degree of NMDAR inhibition and moderate antioxidant activity, while **12** was the most potent NOS inhibitor with moderate VDCC inhibition, low NMDAR inhibition and antioxidant activities. Thus, both **9** and **12** should not be excluded as potential multimodal neuroprotective agents. Compounds **8**, **11** and **12** also had higher calcium modulating activity than NGP1-01 and amantadine. All of these heterocyclic adamantine derivatives (**8**, **9**, **11** and **12**) showed a higher degree of multimodal activity than the previously discussed multimodal neuro-active drugs, amantadine and NGP1-01 (Table 3). Compounds **7** and **10** were the least active derivatives studied with low to

moderate inhibitory potential as calcium modulators, NOS inhibitors and antioxidants. These derivatives are not structurally similar to 7-NI, which might be the reason for low NOS inhibition. Additionally, they do not contain a similar heterocyclic scaffold to the other synthesized derivatives and this could presumably be contributory towards their low activities.

Table 3: Comparison of multifunctional activities of test compounds (o = no/very low activity, x = low activity, xx = moderate activity and xxx = high activity).

Compound	VDCC inhibition	NMDAR inhibition	$DPPH^{\cdot+}$ inhibition	$ABTS^{+}$ inhibition	NOS inhibition
7	o	o	xx	xx	x
8	x	xx	xxx	xxx	xxx
9	o	x	xx	xx	xxx
10	o	xx	xx	o	o
11	xx	xx	x	xx	xxx
12	xx	x	xx	o	xxx
Amantadine	x	x	o	o	o
NGP1-01	xx	x	o	o	o

The synthesised adamantine heterocycles were evaluated for their drug likeliness according to the Lipinski rule of 5 using the online Osiris Property Prediction Software, to elaborate on the potential of these derivatives as drug candidates.[30] The results revealed that all compounds were within the range set by Lipinski (Table 4), in which all four parameter values must be less than five for clogP and H-bond donors and multiples of five for H-bond acceptors and molecular weight. The compounds theoretically should have good absorption and/or permeability properties. The derivatives also have a clogP value of 2 or more and should effectively permeate the BBB.[40] Predicted toxicity studies, as calculated using Osiris, indicated that the synthesized compounds would be free of neurotoxicity, immunotoxicity, reproductive side effects and irritation. This data has significance for the biological activity with interaction on the receptor/enzyme systems, penetration through the cell membrane, BBB permeability and favourable predicted properties during drug metabolism.[41]

Table 4: *In silico* pharmacological parameters for bioavailability and physical/chemical properties of the synthesised compounds.

Compound	Mol formula	Mol weight	Mp(C°)	cLogP[a]	HBD	HBA	Drug score	λ_{ex}[b]	λ_{em}[b]	R_f*
7	$C_{18}H_{24}N_2O$	284	209	3.07 (2.47)	2	1	0.28	366	415	0.56
8	$C_{20}H_{21}NO_3$	324	300	2.20 (1.61)	1	3	0.75	364	407	0.40
9	$C_{18}H_{21}N_3O$	295	212	2.95 (1.30)	2	2	0.44	340	400	0.54
10	$C_{16}H_{19}N_3O_4$	317	300	3.89 (1.59)	3	4	0.62	394	449	0.41
11	$C_{22}H_{28}N_2O_2S$	385	160	4.06 (2.01)	1	4	0.17	334	517	0.59
12	$C_{19}H_{20}N_2$	276	160	4.75 (0.15)	0	2	0.28	358	395	0.79

*R_f = EtOAc:Acetone 2:1
[a]Values in brackets indicate the cLogP of the free heterocyclic moieties
λex = excitation λ; λem = emission λ.
[b]At 10^{-5} M in absolute ethanol at 25 °C.

6.4. Conclusion

Excess accumulation of calcium in neuronal cells rapidly leads to cell death through a variety of mechanisms, including activation of proteases, nucleases, phospholipases, nitric oxide synthase (NOS), and other degradative enzymes that not only lead to the activation of cell death cascades, but also to free radical formation.[26,27] The test compounds were evaluated for VGCC-, NMDAR- and NOS inhibition and antioxidant activity. The potential to increase dopamine transmission is also postulated because of the amantadine moiety in all structures. The results showed that the heterocyclic adamantane amine structures have a high degree of inhibitory activity on VGCC, NMDAR and NOS and demonstrated radical scavenging activity in the $DPPH^{\cdot+}$ and $ABTS^{+}$ assays.

The derivatives with polyaromatic functionalities in their structures exhibited an increased degree of multifunctionality when compared to those with mono-aromatic structures. The compounds all contained amide or amine functionalities linking the two functional moieties and the coumarin and dansyl compounds in general had the best activity in the series. Using these privileged structures and utilizing bioisosteric substitution of the amine and amide functions, an extended series of compounds could be synthesised to further develop structure activity relationships in this series of fluorescent compounds.

These compounds can thus be considered as potential multifunctional neuroprotective agents and may serve as new lead structures in the search for active therapeutics. Although these derivatives under study were found to be neuroprotective agents, their potential beneficial effects and safety in humans needs to be proven and further *in vivo* studies need to be conducted to elaborate on the true potential of these derivatives. An additional benefit of these

derivatives is that they may also be utilized in the development of fluorescent displacement and other pharmacological studies. This could provide critical information about the neurodegenerative processes and replace the use of traditional and hazardous radioligand binding studies. The potential of these fluorescent heterocyclic compounds should therefore be further explored as multifunctional neuroprotective drugs with favourable physical chemical properties and/or as fluorescent ligands in biological assay development.

6.5. Experimental

6.5.1 Chemistry: general procedures

Unless otherwise specified, materials were obtained from Sigma Aldrich® and Merck® and used without further purification. All reactions were monitored by thin-layer chromatography on 0.20 mm thick aluminium silica gel sheets (Alugram® SIL G/UV_{254}, Kieselgel 60, Macherey-Nagel, Düren, Germany). Visualisation was achieved using a Chromato-vue® Cabinet under UV light (254 nm and 366 nm) or with iodine vapours. Mobile phases were prepared on a volume-to-volume basis. Infra red (IR) spectra were recorded on a Perkin Elmer Spectrum 400 spectrometer, fitted with a diamond attenuated total reflectance (ATR) attachment. Mass spectra (MS) were recorded on an analytical VG 70-70E mass spectrometer using electron ionisation (EI) at 70 eV. The MS of **8** and **11** were recorded on a Thermo Electron LXQ ion trap mass spectrometer with atomic pressure chemical ionisation (APCI) source set at 70 eV. A Themo Electron DFS magnetic sector mass spectrometer at 70 eV and 250 °C was used to obtain high resolution electron impact (HREI) mass spectra for compounds **7**, **8**, **9**, **10** and **12**. HREI mass spectra for compound **11** were recorded on a Waters API Q-Tof Ultima mass spectrometer at 70 eV and 100 °C. All HREI samples were introduced by a heated probe and perfluorokerosene was used as reference standard. Melting points were determined using a Stuart SMP-300 melting point apparatus in capillary tubes and are uncorrected. ^{1}H and ^{13}C NMR spectra were obtained using a Varian Gemini 200 spectrometer at a frequency of 200 MHz and 50 MHz, respectively. ^{1}H and ^{13}C spectra for compound **8** were obtained from a Bruker Advanced 600 Spectrometer at frequencies of 600 MHz and 150 MHz respectively. Tetramethylsilane (TMS) was used as a point of reference in all NMR experiments. All chemical shifts are reported in parts per million (ppm) relative to the signal from TMS ($\delta = 0$), added to an appropriate deuterated solvent. The following abbreviations are used to describe the multiplicity of the respective signals: s

(singlet), br s, (broad singlet), d (doublet), dd (doublet of doublets), t (triplet), q (quartet) or m (multiplet).

6.5.2 Synthesis

The synthetic procedures employed in the study followed two chemical pathways: amidation using *N,N*-carbonyldiimidazole (CDI) as activation agent and direct amination. Compounds **7**, **9**, **10** and **12** were synthesized using methods as previously described with modifications to improve yield and purity.[28] The well described pentacycloundecane derivative NGP1-01 (**3**) was synthesized according to published methods and the physical characteristics was identical too previously described.[17-23]

6.5.2.1. *N*-Adamantan-1-yl-2(methylamino)-benzamide (7): *N,N*-carbonyldiimidazole (0.33 g, 2.035 mmol) was added to a solution of *N*-methylanthranilic acid (0.28 g, 1.85 mmol) in tetrahydrofuran (10 mL). The resulting solution was protected from light and stirred at room temperature for 24 hours. A solution of amantadine hydrochloride (0.280 g, 1.85 mmol) in tetrahydrofuran (10 mL) and triethylamine (0.615 g) was added slowly. The resulting solution was protected from light and stirred for 48 hours at room temperature. The reaction mixture was added to water and extracted with DCM (3 x 100 mL). The organic phase was collected, dried ($MgSO_4$) and the solvent was removed *in vacuo* rendering the product as a yellow oil. The yellow oil was added to ethyl acetate and a precipitate formed upon standing. The precipitate was filtered and washed with cold ethyl acetate (2 x 15 mL), yielding the product as a light-yellow amorphous solid (0.388 g, 1.35 mmol, 73%). ***Physical data:*** $C_{18}H_{24}N_2O$; **mp:** 213°C; **^{1}H NMR** (200 MHz, $CDCl_3$) δ_H: 8.01-7.97 (dd, J = 6.5 and 2.2 Hz,1H), 7.28 (m, 2H), 6.56-6.62 (m, 3H), 2.86 (s, 3H), 2.00 (s, 3H), 1.86 (d, 6H), 1.62-1.44 (m, 6H); **^{13}C NMR** (50 MHz, $CDCl_3$) δ_C: 175.01, 151.75, 132.74, 132.49, 117.54, 113.96, 110.05, 51.09, 40.98, 35.80, 29.74, 29.12; **MS** (EI, 70 eV) *m/z*: 284 (M^+). **HREI-MS**: Calculated for $C_{18}H_{24}N_2O$ (MH^+); 284.18889, found 284.18864. **IR** (ATR) ν_{max}: 3341, 2911, 2853, 1609, 1503, 1365, 754.

6.5.2.2. *N*-(1-Adamantyl)-2-oxo-chromene-3-carboxamide (8): One portion of *N,N*-carbonyldiimidazole (0.33 g, 2.035 mmol) was added to a solution of coumarin-3-carboxylic acid (0.352 g, 1.85 mmol) in DMF (10 mL). The resulting solution was stirred at 60°C for 24 hrs, after which a solution of amantadine hydrochloride (0.28 g, 1.85 mmol), in DMF (5 mL) and triethylamine (0.77 mL) was added. The resulting solution

was stirred for 24 hrs under reflux conditions. The crude product was added to DCM, extracted from water acidified with 32% HCl to pH 3. The water phase was basified with 1 *N* NaOH (pH 12) and extracted with DCM (2 x 25 mL). The combined organic layers were removed *in vacuo* rendering the crude product as a white solid. The solid was recrystallized from ethanol, rendering the pure product as a white crystalline solid (0.300 g, 0.93 mmol, 50%). ***Physical data:*** $C_{20}H_{21}NO_3$; **mp:** 300°C; **^{1}H NMR** (600 MHz, $CDCl_3$) δ_H: 8.90 (s, 1H,), 7.71-7.62 (m, 2H), 7.41-7.33 (m, 2H), 2.05 (s, 3H), 1.75-1.64 (m, 12H); **^{13}C NMR** (150 MHz, $CDCl_3$) δ_C: 161.60, 159.89, 154.30, 147.64, 133.69, 129.64, 125.13, 119.53, 118.72, 116.48, 52.28, 41.35, 36.34, 30.88, 29.39. **APCI-MS** (300°C, 70 eV) *m/z*: 324.16 (M^+); **HREI-MS**: Calculated for $C_{20}H_{21}NO_3$ (MH^+); 323.15159, found 323.15214. **IR** (ATR) ν_{max}: 3341, 2911, 2853, 1609, 1503, 1365, 754.

6.5.2.3. *N*-Adamantan-1-yl-1*H*-indazole-3-carboxamide (9): *N,N*-carbonyldiimidazole (0.33 g, 2.035 mmol) was added to a solution of 1*H*-indazole-3-carboxylic acid (0.3 g, 1.85 mmol) in DMF (20 mL). The resulting solution was protected from light and heated to 60°C for 24 hrs and then cooled to room temperature before adding a solution of amantadine hydrochloride (0.280 g, 1.85 mmol) in tetrahydrofuran (10 mL) and triethylamine (0.615 g). The resulting solution was protected from light and stirred for 48 hours at room temperature. Thereafter, the precipitate was filtered and washed with cold tetrahydrofuran (2 x 15 mL), yielding the crude product as a white amorphous solid. Further purification *via* flash column chromatography (10% hexane:ethyl acetate) yielded the compound as a white solid. The product was recrystallized from ethanol, rendering the title compound as a white crystalline solid (0.315 g, 1.07 mmol, 52.5%). ***Physical data:*** $C_{18}H_{21}N_3O$; **mp:** 212°C **^{1}H NMR** (200 MHz, MeOD) δ_H: 8.26-8.22 (dd, J = 6.5 and 2.2 Hz,1H), 7.54-7.50 (dd, J = 6.5 and 2.2 Hz, 1H), 7.38-7.31 (m, 1H), 7.22-7.14 (m, 1H), 2.14 (s, 3H), 1.88 (d, 6H), 1.74-1.72 (m, 6H); **^{13}C NMR** (50 MHz, MeOD) δ_C: 170.65, 162.00, 143.29, 127.35, 123.73, 123.66, 122.58, 111.38, 52.64, 47.78, 41.60, 36.51, 30.48; **MS** (EI, 70 eV) *m/z*: 295 (M^+); **HREI-MS**: Calculated for $C_{18}H_{21}N_3O$ (MH^+); 295.36880, found 295.36699. **IR** (ATR) ν_{max}: 2979, 2909, 2854, 1637, 1475, 1322, 809, 733.

6.5.2.4. *N*-(2,4-Dinitrophenyl)adamantan-1-amine (10): 1-Fluoro-2,4-dinitrobenzene (0.233 g, 1.25 mmol) and amantadine hydrochloride (0.235 g, 1.25 mmol) were dissolved in 25 mL absolute acetonitrile. Triethylamine (0.378 g, 3.73 mmol) was added to the reaction mixture. The reaction mixture was stirred under reflux conditions in darkness for 48 hours.

Thereafter the precipitate was filtered to obtain the crude product as a bright yellow amorphous solid. Further purification with flash column chromatography (10% hexane:ethyl acetate) yielded the compound as a light yellow solid (0.368 g, 1.16 mmol, 93%). ***Physical data:*** $C_{16}H_{19}N_3O_4$; **mp:** 300°C; **^{1}H NMR** (200 MHz, $CDCl_3$) δ_H: 9.18-9.12 (d, 1H, J = 2.2 Hz), 8.81 (s, 1H, NH), 8.23-8.12 (dd, 1H, J = 5.1 and 2.2 Hz), 7.25-7.20 (d, 1H, J = 5.1 Hz), 2.23 (s, 3H), 2.18-2.08 (m, 6H), 1.82-1.73 (m, 6H); **^{13}C NMR** (50 MHz, $CDCl_3$) δ_C: 147.86, 135.51, 131.02, 129.28, 129.28, 124.97, 116.305, 29.56, 36.15, 42.20, 54.34; **MS** (EI, 70 eV) *m/z*: 317 (M^+); **HREI-MS**: Calculated for $C_{16}H_{19}N_3O_4$ (MH^+); 317.13802, found 317.13756. **IR** (ATR) ν_{max}: 3321, 3107, 2927, 2857, 1621, 1587, 1335, 1088, 916, 743.

6.5.2.5. *N*-Adamantan-1-yl-5-dimethyl-amino-1-naphthalenesulfonic acid (11): Dansyl chloride (0.5 g, 1.85 mmol) in chloroform (10 mL) was added drop-wise to a solution of amantadine hydrochloride (0.28 g, 1.85 mmol) and triethylamine (0.77 ml) in chloroform (5 mL) and stirred for 48 hours. The reaction mixture was washed successively with 10% Citric acid (5×10 mL), 10% $NaHCO_3$ (5×10 mL) and water (3×10 mL), dried with $MgSO_4$ and concentrated *in vacuo*. Purification with flash column chromatography (30% hexane:ethyl acetate) yielded the crude compound as a yellow oil. The oil was further purified by recrystallisation from chloroform and a few drops of *n*-Hexane. The light yellow crystals were washed with cold cyclohexane (2×15 mL) to produce the product as a white-yellowish crystalline solid (0.250 g, 0.65 mmol, 35%). ***Physical data:*** $C_{22}H_{28}N_2O_2S$; **mp:** 160°C; **^{1}H NMR** (200 MHz, $CDCl_3$) δ_H: 8.64-8.59 (dd, J = 6.2 and 2.2 Hz, 1H), 8.40-8.36 (dd, J = 6.3 and 2.2 Hz, 1H) 8.28-8.24 (dd, J = 6.3 and 2.1 Hz, 1H), 7.78 (br s, 1H, NH), 7.54-7.40 (m, 2H), 7.13-7.09 (dd, J = 6.4 and 2.1 Hz, 1H), 2.85 (s, 6H, $N(CH_3)_2$) 1.86 (s, 3H), 1.71 (d, 6H),1.50-1.28 (m, 6H); **^{13}C NMR** (50 MHz, $CDCl_3$) δ_C: 181.38, 140.35, 130.46, 129.92, 127.74, 127.21, 126.34, 123.61, 121.70, 114.69, 52.68, 45.53, 40.12, 35.38, 28.99. **APCI-MS** (300°C, 70 eV) *m/z*: 384.20 (M^+). **HREI-MS**: Calculated for $C_{22}H_{28}N_2O_2S$ (MH^+); 385.1950, found 385.1944. **IR** (ATR) ν_{max}: 3290.86, 2902.11, 2849.28, 2779.45, 1614.28, 1588.52, 1577.02, 1438.47, 1308.27, 1143.95, 1086.98, 783.93

6.5.2.6. *N*-(1-Cyano-2*H*-isoindol-2-yl)adamantan-1-amine (12): Amantadine hydrochloride (0.6 g, 3.301 mmol) and sodium cyanide (NaCN) (0.132 g, 3.301 mmol) was dissolved in 20 ml of methanol. Distilled water (1 mL) was added and the mixture was stirred until all the NaCN dissolved (± 15 minutes). *o*-Phthaldialdehyde (0.442 g, 3.301 mmol) was dissolved in 10 mL methanol and added drop-wise (± 10 minutes) to the reaction mixture. A white

precipitate formed almost immediately. The reaction mixture was protected from light and stirred at room temperature for 24 hrs to ensure completion of the reaction. The precipitate was filtered and washed twice with cold methanol to yield the crude product as a white amorphous solid. The crude product was dissolved in DCM, which was then extracted with acidified water of pH 3. The water phase was basified with 5 *N* NaOH (pH 12) and extracted with DCM (2 x 25 mL). The organic phase was removed *in vacuo* rendering the crude product as a white solid. Crystallization from THF/Ethanol (2:1) rendered the pure product as colourless crystals (0.600 g, 2.17 mmol, 66%). ***Physical data:*** $C_{19}H_{20}N_2$; **mp:** 160°C; **^{1}H NMR** (200 MHz, $CDCl_3$) δ_H: 7.69-7.64 (m, 2H), 7.51 (s, 1H), 7.26-7.19 (m, 1H), 7.12-7.04 (m, 1H), 2.45 (m, 6H), 2.32 (s, 3H), 1.83 (m, 6H); **^{13}C NMR** (50 MHz, $CDCl_3$) δ_C: 150.64, 133.86, 125.34, 122.74, 122.39, 120.88, 117.83, 166.59, 115.88, 60.43, 43.00, 35.97, 30.03; **MS** (EI, 70 eV) *m/z*: 276 (M^+); **HREI-MS**: Calculated for $C_{19}H_{20}N_2$ (MH^+); 276.16366, found 276.16265. **IR** (ATR) ν_{max}: 3140, 2910, 2850, 2189, 1182, 783, 752.

6.6. Biological evaluations

6.6.1. Materials

All chemicals used were of analytical or spectroscopy grade and were purchased from Merck (St Louis, MO, USA) and Sigma-Aldrich® (UK).

6.6.2. Animals

The study protocol was approved by the Ethics Committee for Research on Experimental Animals of the North-West University (Potchefstroom Campus). Male Spraque-Dawley rats were sacrificed by decapitation and the brain tissue was removed and kept on ice for homogenation. After homogenation, the alliquoted brain homogenate was snap freezed with liquid N_2 and stored at -70 °C.

6.6.3. Imaging experiments using Mag-fura-2AM

6.6.3.1. Methods

The fluorescent ratiometric indicator, Mag-Fura-2/AM, and a Cary-Eclipse® fluorescence spectrometer were used to evaluate the influence of the test compounds on calcium homeostasis *via* the VDCC and NMDA receptor channels utilizing murine synaptoneurosomes. Preparation of synaptoneurosomes, solutions and experimental

techniques were similate to those of published studies.[42,43] All data analysis, calculation and graphs were done using Prism 4.02® (GraphPhad, Sorrento Valley, CA). Data analysis was carried out using the Student Newman Keuls multiple range test and the level of significance was accepted at $p < 0.05$.

6.6.3.2. Preparation of Synaptoneurosomes

Male adult Sprague-Dawley rats were used. Rats were sacrificed by decapitation, and the whole brains were removed. Whole-brain synaptoneurosomes were prepared by the techniques of Hollingsworth *et al*,[33] modified slightly. The brains from 2 rats were homogenized (4 strokes by hand using a homogenizer) in 30 ml of ice-cold Krebs-bicarbonate buffer (NaCl, 118 mM; KCl, 4.7 mM; MgCl, 1.18 mM; $CaCl_2$ 1.2 mM; $NaHCO_3$ 24.9 mM; KH_2PO_4 1.2 mM; and glucose, 10 mM). From this step forward the homogenate was kept ice-cold at all times to minimize proteolysis throughout the isolation procedure. The tissue suspension was placed in a 50 ml polycarbonate tube and then centrifuged for 15 min at 1100 x g and 0 °C. After centrifugation, the pellet was resuspended by hand in 30 ml fresh incubation buffer using a Pasteur pipette and then centrifuged again as described above. Directly after centrifugation the pellet was gently resuspended in Krebs-bicarbonate buffer at a protein concentration (measured spectrofluorimetrically) of 3 mg/ml. Protein yield was about 10 mg/g tissue.

6.6.3.3. General procedure for loading FURA-2AM and incubating test compounds

Experiments were carried out at 37°C and fluorescence was measured with a spectrofluorimeter (Cary-Eclipse® fluorescent spectrometer) equipped with a water-jacketed cuvette holder. The synaptoneurosome suspension prepared above was allowed to reach room temperature, thereafter Fura-2 AM (5 mM in DMSO – protect solution from light) was added to produce a final concentration of 5 μM. Synaptoneurosomes were then incubated at 37°C for 10 min, diluted with Krebs-bicarbonate buffer at room temperature to a final concentration of 0.6 mg/mL and kept at room temperature until and protected from light. Immediately before the experiment, 0.25 ml of the Fura-2 AM synaptoneurosomal suspension was centrifuged for 10 sec in a desk Hermle Z 100 M® Microfuge. The supernatant was discarded and the pellet was resuspended in 0.75 ml of 37°C Krebs-HEPES buffer (20 mM HEPES substituting for $NaHCO_3$ and adjusted with NaOH to pH 7.4). HEPES buffer was used instead of bicarbonate buffer because the latter causes the appearance of bubbles in the cuvette and thus increased

the "noise." For the screening test 100 mM stock solutions of the compounds in DMSO (final DMSO concentration in the incubations = 0.1%) was prepared. The stock solution (0.75 µl) was diluted in the 0.75 ml Krebs-HEPES buffer solution as prepared above to give 100 µM concentrations of the compounds. Control experiments received 0.1% DMSO to compensate for possible alterations caused by addition of DMSO in experiments.

6.6.3.4. KCl mediated calcium stimulation

The wavelengths selected were 344 nm (excitation) and 506 nm (emission). The optics position was set at the bottom and sensitivity set at 100 with a runtime of 40 seconds with 150 msec intervals. The test compound was incubated for 5 min at 37°C and used immediately after incubation. The procedure was initiated and kept at 37°C. At 10 seconds into the recording 100 µl of KCl (140 mM) depolarization solution (43 mM NaCl, 140 mM KCl, 10 mM $NaHCO_3$, 1.4 mM $CaCl_2$, 0.9 mM $MgSO_4$, 5.5 mM Glucose, and 20 mM HEPES. pH adjusted to 7.4 with NaOH) was added to the membrane preparation to depolarize the synaptoneurosomes and activate the calcium mediated calcium flux. Addition was done at the side of the cuvette, taking care not to disturb the surface that would consequently create a disturbance in the optical effect. Experiments were repeated three times on different tissue preparations with three determinations in each replicate.

6.6.3.5. NMDA/Glycine mediated calcium stimulation

The selected wavelengths were 344 nm (excitation) and 506 nm (emission). The optics position was set at the bottom and sensitivity set at 100 with a runtime of 40 seconds with 150 msec intervals. The test compound was incubated for 5 min at 37°C and used immediately after incubation. The procedure was initiated and kept at 37°C, at 10 seconds into the recording 100 µl of krebs-HEPES buffer containing NMDA (100 µM) and Gly (100 µM) was added to the membrane preparation (Addition was done at the side of the cuvette, taking care not to disturb the surface that would consequently create a disturbance in the optical effect). The addition of NMDA (100 µM) and Gly (100 µM) resulted in activation of NMDAR mediated calcium flux. Experiments were repeated three times on different tissue preparations with three determinations in each replicate.

6.6.4. NOS inhibition assay

6.6.4.1. Methods

Spectrophotometric scans were recorded using a Varian Cary-50® UV-Visible spectrophotometer. The slope values were calculated at specific wavelengths and calculated from the inhibition data. All data analysis, calculation and graphs were done using Prism 4.02® (GraphPhad, Sorrento Valley, CA). Data analysis was carried out using a one-way analysis of variance, followed by the Student-Newman-Keuls multiple range test. The level of significance was accepted at $p < 0.05$.

NOS assay procedure: HEPES buffer (100 mM) was prepared by dissolving the HEPES in double-distilled water and adjusted to pH 7.4 by the addition of 4 N NaOH at 37 °C. The extraction buffer was prepared by dissolving sucrose (320 mM), HEPES (20 mM), and ethylenediamine tetra-acetic acid (1 mM) in double-distilled water and adjusting the pH to 7.4 at room temperature by addition of 10% HCl.[44] The following constituents were then added to the final concentrations indicated: 0.1 mM D/L dithiotherol (DTT), 0.5 µM leupeptin, soybean-trypsin inhibitor (10 µg/ml) and aprotin (2 µg/ml). The extraction buffer was prepared to its final volume with distilled water and distributed into aliquots (typically 50 ml per aliquot) and stored at -20°C until required. Phenylmethylsulphonyl fluoride (PMSF; 10 mg/ml) is unstable in aqueous solution and was not included in the buffer at this stage, but prepared as a solution in absolute ethanol, stored at -20°C, and added to the extraction buffer during the extraction procedure. The composition of the extraction buffer is designed to permit extraction of NOS from tissues without breaking intracellular organelles and to minimise proteolysis.[45] Extractions and storage of tissue samples prior to the assay were carried out at 0 – 4°C to avoid loss of enzyme activity. Fresh rat brain was weighed in 50 ml pre-cooled Falcon tubes and placed on ice. After rinsing with ice cold extraction buffer, a measured volume of extraction buffer (5 ml/g tissue) was added to the tissue. The sample was then homogenised with a mechanical homogeniser while the temperature was maintained at < 4 °C. After 10 seconds of homogenisation the PMSF (10 µM/ml of extraction buffer) was added to the mixture and it was homogenised for a further 30 seconds. The homogenate was then centrifuged at 12 000 x g for 10 minutes. Once the supernatant was collected, it was divided into 2 ml aliquots which were assayed immediately or snap freezed and stored at -70 °C. The oxyhemoglobin solution was prepared by carefully dissolving the hemoglobin crystals (25 mg) in 1000 µl of cold HEPES buffer and subsequent reduction with excess

sodium dithionate (0.958 mg). The solution immediately changed from brownish red (mixture of oxyHb and metHb) to a dark red (deoxyhemoglobin) colour after the reductant was added. Oxygenation was carried out by passing 100% oxygen over the surface while the solution was gently swirled for 15 minutes. The gradual colour change from dark red to bright red was indicative of the oxygenation of hemoglobin. Desalting and purification was performed by passing the resulting oxyHb solution through a Sephadex G-25 column. The oxyHb was eluted as a single bright-red band. The front and back edges were discarded. The concentration of oxyHb was calculated by methods described by Feelisch[46] and Hevel.[47,48] 10 µl of the oxyHb stock solution was added to 2990 µl of HEPES buffer in a cuvette and the absolute absorbance was determined in triplicate at 415 nm against a blank buffer. The concentration of oxyHb (C_{oxyHb}) was calculated with the following equation (1) using a molar extinction coefficient $E_{415(oxyHb)}$ of 131.0 mM^{-1} cm^{-1}.

$$C_{oxyHb} = \frac{A415nm \times 300 \text{ (dilution factor)}}{E_{415(oxyHb)}} \quad (1)$$

The stock solution was then aliquoted in 200 µl units, snap freezed with liquid N_2 and stored at -70°C. Calcium chloride solution ($CaCl_2$; 12.5 mM), *L*-arginine (1 mM) and NADPH (5 mM) were prepared in HEPES buffer. The test compounds were dissolved in DMSO and the concentration of the organic solvent did not exceed 2% of the final incubation concentrations. This gave a series of concentrations in the micro molar range. Oxyhemoglobin, $CaCl_2$, *L*-arginine and the test compound were then diluted in the HEPES buffer to give final concentrations of 250 µM $CaCl_2$ and 1 mM *L*-arginine. The reaction mixture was prewarmed for three minutes to the required assay temperature of 37°C and the reaction was started by the addition of NADPH and the tissue extract (100 µl) (in the form of rat brain homogenate) with a final NADPH concentration of 100 µM. After establishing the baseline, continuous scans with a scan rate of 600 nm/min every 10 seconds were recorded between 390 nm and 430 nm. The conversion of oxyHb to metHb was monitored over a period of 10 minutes. The increase in the molar amount of metHb correlates to the molar amount of NO generated from the NOS enzyme.

6.6.5. $ABTS^+$ and $DPPH^{\cdot+}$ assays

6.6.5.1. Methods

Assay absorbance measurements were recorded using a Cintral 202® UV-vis spectrophotometer at specific wavelengths as elaborated below. The experimental data was analysed using Prism 4.02® (GraphPhad, Sorrento Valley, CA) and Microsoft Excel 2007.

6.6.5.2. $ABTS^+$ radical scavenging assay

$ABTS^+$ radical cations were produced by reacting $ABTS^+$ (7 mM) in 5 mL water with potassium persulfate (2.45 mM) and incubating the mixture at room temperature in the dark for 16 h.[49-51] The solution thus obtained was further diluted with absolute ethanol to give an absorbance of 0.7 in a 1 cm cuvette ($ABTS^+$ working solution). Different concentrations of the test sample in 200 µl DMSO were added to 1.8 mL of $ABTS^+$ working solution to give final volumes of 2 mL. After 30 min of incubation at room temperature the absorbance was recorded at 734 nm. DMSO (200 µl) without test compound served as the standard and was taken as 100% activity of $ABTS^+$. For statistical viability, the assay was performed three times with 3 readings for each concentration. The known antioxidant Trolox® was used as reference standard. The percentage inhibition was calculated from the following equation (2):

% inhibition = [(Absorbance of control – Absorbance of test sample)/Absorbance control] x100 (2)

6.6.5.3. $DPPH^{\cdot+}$ radical scavenging activity

Antioxidant scavenging activity was studied using 1,1-diphenyl-2- picrylhydrazyl free radical ($DPPH^{\cdot+}$).[52,53] Various concentrations of test solutions in 200 µl DMSO were added to 1.8 mL of 0.1 mM solution of $DPPH^{\cdot+}$ in methanol. Neat methanol (0.2 mL) was used as experimental control. After 30 min of incubation at room temperature, the reduction in the number of free radical was measured by reading the absorbance at 517 nm. Trolox® was used as reference standard. The scavenging activity of the samples corresponded to the intensity of the quenching of $DPPH^{\cdot+}$. For statistical viability, the assay was performed three times with 3 readings for each concentration. The percentage inhibition was calculated from the following equation (3):

% inhibition = [(Absorbance of control – Absorbance of test sample)/Absorbance control] x100 (3)

6.7. Statistical analysis

All data analysis, calculation and graphs were done using Prism 4.02® (GraphPhad, Sorrento Valley, CA). Data analysis was carried out using the Student Newman Keuls multiple range test of test compounds versus controls. The level of significance was accepted at $p < 0.05$. Bonferroni's Multiple Comparison, one way analysis of variance (ANOVA) was performed on selected data to indicate significant differences between test compounds ($p < 0.05$ was considered to be a statistically significant difference).

6.8. *In silico* pharmacological property and SAR study

The pharmacological properties of the compounds such as molecular weight, cLogP HBA, HBD, ionization potential, drug score and drug likeness of the compounds were studied using the online Osiris Property Explorer (http://www.organic-chemistry.org/prog/peo/)[54] for drug bioavailability of chemical compounds.[32]

6.9. Fluorescence spectrometry

A Cary Eclipse® fluorescence spectrometer was used for fluorescence measurements. The fluorescent compounds were measured at a concentration of 10^{-5} M in absolute ethanol at room temperature. Emission spectra were recorded at the excitation maximal wavelength.

Acknowledgments

We are grateful to the University of the Western Cape, North-West University, Medicine Research Council and the National Research Foundation for financial support. We would also like to acknowledge the contribution of the 2010 Pharmaceutical Chemistry, Undergraduate Research Group at the University of the Western Cape.

Supplementery data

^{1}H-NMR and ^{13}C-NMR spectra for all synthesised compounds are presented in Annexure E

References

1. Rang H.P.; Dale M.M.; Ritter J.M. Rang and Dale's Pharmacology, Elsevier, Philadelphia. 2007, chap.35, pp. 508.
2. Dawson, T.M.; Dawson, V.L. Nature. Neurosc. Suppl. 2002, 5, 1058.

3. Araki, T.; Kumagai, T.; Tanaka, K.; Matsubara, M.; Kato, H.; Itoyama, Y.; Imai, Y. Brain research. 2001, 918, 176.
4. Kemp, J.A.; Mckernan, R.M. Nat. Neurosci. Suppl. 2002, 5, 1039.
5. Mattson, M.P. Neuromol. Med. 2003, 3, 65.
6. Meldrum, B.; Garthwaite, J. Trends Pharmacol. Sci. 1990, 11, 379.
7. Alexi, T.; Borlogan, C.V.; Faull, R.L.M.; Williams, C.E.; Clark., R.G.; Gluckman, P.D.; Huges, P.E. Progr. Neurobiol. 2000, 60, 409.
8. Cano-Abad, M.F.; Villarroya, M.; Garcia, A.G.; Gabilan, N.H.; Lopez, M.G. J. Biol. Chem. 2001, 276, 39695.
9. Moncada, S.; Palmer, R.M.J.; Higgs, E.A. Biochem. Pharmacol. 1989, 38, 1709.
10. Hibbs, J.B., Jr.; Vavrin, Z.; Taintor, R.R. J. Immunol. 1987, 138, 550.
11. Prins, L.H.A.; Petzer, J.P.; Malan, S.F. Bioorg. Med. Chem. 2009, 17, 7523.
12. Van der Schyf, C.J.; Geldenhuys, W.J.; Youdim, M.B.H. J. Neurochem. 2006, 99, 1033.
13. Jellinger, K. A. J. Neural. Transm. 2003, 65, 101.
14. Mizoguci, K.; Yokoo, H.; Yoshida, M.; Tanaka, T.; Tanake, M. Brain Res.1994, 662, 255.
15. Danysz, W.; Parsons, C.G.; Kornhuber, J.; Schmidt, W.J.; Quack, G. Neurosci. Biobehav. Rev. 1997, 21, 455.
16. Parsons, C.G.; Danysz, W.; Quack, G. Neuropharm. 1999, 38, 735.
17. Zou, J.Y.; Crews, F.T. Brain. Res. 2005, 1034, 11.
18. Van der Schyf, C.J.; Squier, G.J.; Coetzee, W.A. Pharmacol. Res. Commun. 1986, 18, 407.
19. Geldenhuys, W.J.; Malan, S.F.; Bloomquist, J.R.; Van der Schyf, C.J. Bioorg. Med. Chem. 2007, 5, 1525.
20. Kiewert, C.; Hartmann, J.; Stoll, J.; Thekkumkara, T.J.; Van der Schyf, C.J.; Klein, J.; Neurochem. Res. 2006, 31, 395.
21. Mdzinarishvili, A.; Geldenhuys, W.J.; Abbruscato, T.J.; Bickel, U.; Klein, J.; Van der Schyf, C.J. Neurosci. Lett. 2005, 383, 49.
22. Geldenhuys, W.J.; Malan, S.F.; Murugesan, T.; Van der Schyf, C.J.; Bloomquist, J.R. Bioorg. Med. Chem. 2004, 12, 1799.
23. Geldenhuys WJ, Terre'Blanche G, Van der Schyf CJ, Malan SF. Screening of novel pentacycloundecylamines for neuroprotective activity. Eur. J. Pharmacol. 2003, 458, 73.
24. Zheng, H.; Youdim, M.B.; Fridkin, M. J. Med. Chem. 2009, 52, 4095.

25. Neuraxon, Inc. 1,5 and 3,6-substituted indole compounds having NOS inhibitory activity. WO2007118314; 2007
26. Van der Schyf C.J.; Youdim, M.B.. Neurother. 2009, 6, 1-201.
27. Youdim, M.B.H. Rambam Maimonides Medical Journal. 2010, 1(2), 1
28. Joubert, J., Van Dyk, S., Malan, S.F. Bioorg. Med. Chem. 2008, 16, 8952.
29. Tsuzuki, N., Hama, T.; Kawada, M.; Hasui, A.; Konishi, R.; Shiwa, S.; Ochi, Y.; Futaki, S.; Kitagawa, K. J. Pharm. Sci. 1994, 83(4), 481.
30. Moncada, S.J.; Palmer, R.M.; Higgs, E.A. Pharmacol. Rev. 1991, 43, 109.
31. Handy, R.L.C.; Wallace, P.; Gaffen, Z.A.; Whitehead, K.J.; Moore, P.K. Br. J. Pharmacol. 1995, 116, 2349.
32. Lipinski, C. A. Drug. Discover. Today. 2004, 1, 337.
33. Hollingsworth, E.B.; McNeal, E.T.; Burton, J.L.; Williams, R.J.; Daly, J.W. Creveling, C.R. J. Neurosci. 1985, *5,* 2240-2253.
34. Crawley, J.N.; Gefen, C.R.; Rogawski, M.A.; Sibley, D.R.; Skolnick, P.; Wray, S. *Current protocols in neuroscience.* 2001, Retrieved 3 June 2008, from https://commerce.invitrogen.com/index.cfm?fuseaction=iProtocol.unit SectionTree&treeNode=9E663C86A2A3FA409F26D8F850F50254
35. Salter, M.; Knowles, R. G. Methods in molecular biology. In: Nitric Oxide Protocols; Titheradge, M. A., Ed.; Humana Press: Totowa, NJ, 1996; Vol. 100, pp 61–65
36. Salter, M.; Knowles, R. G.; Moncada, S. FEBS Lett. 1991, 291, 145.
37. Nishida, J.; Kawabata, J. Biosci. Biotechnol. Biochem. 2006, 70, 193–202.
38. Velavan, S.; Naghlendran, K.; Mahesh, R.; Hazeena B. V. *PHCOGMAG*, 1998, ISSN: 0973-1296.
39. Karali, N.; Guzel, O.; Ozsoy, N. Ozbey, S. Salman, A. Euro. J. Med. Chem. 2010, 45, 1068.
40. Silverman, R.B., The organic chemistry of drug design and drug action. 2nd Eds.; Elsevier.: London, 2004; pp 1-617.
41. Stanchev, S.; Momekov, G.; Jensen, F. Eur. J. Med. Chem. 2008, 43, 694.
42. Resch, K.; Imm, W.; Ferber, E.; Wallach, D. F. H.; Fischer, H. Naturwissenschaften 1971, 58, 220.
43. (a) Benavide S, J.; Claustre, Y.; Scatton, B. Journal of Neuroscience. 1988, 8(10), 3607. (b) Bezuidenhout, L-M. Triquinylamine as regulators of calcium homeostasis of neuronal cells. Pharmaceutical sciences. 2007. Potchefstroom, North West University. M.sc.: 154. (c) Crawley, J. N.; Gefen, C. R.; Rogawski, M. A.; Sibley, D. R.; Skolnick, P.; Wray, S.

Current protocols in neuroscience. 2001. Retrieved 3 June 2008, from https://commerce.invitrogen.com. (d) Geldenhuys, W. J.; Malan, S. F.; Bloomquist, J. R.; Van der Schyf, C. J. Bioorganic and Medicinal Chemistry. 2007, 15, 1525. (e) Lambert, D. G., Ed. Calcium signaling protocols. 1999. Methods in molecular biology. Totowa, New Jersey, Humana Press. (f) Resch, K.; Imm, W.; Ferber, E.; Wallach, D. F. H.; Fischer, H. Naturwissenschaften. 1971, 58, 220. (g) Stout, A. K. and I. J. Reynolds. Neuroscience. 1999, 89(1), 91. (h) Takahashi, A. P.; Camacho, E.A. Physiol Rev. 1991, 79(4), 1089.

44. Corbett, J. A.; McDaniel, L. M. Methods Enzymol. 1996, 10, 21.
45. Dawson, J.; Knowles, R. G. Mol. Biotechnol. 1999, 12, 275.
46. Feelish, M.; Kubitzek, D.; Werringloer, J. The oxyhemoglobin assay. In Methods in Nitric Oxide Research; Feelish, M., Stamler, J. S., Eds.; Wiley & Sons Ltd.: London, 1996; pp 455–478.
47. Hevel, J. M.; Marletta, M. A. Methods. Enzymol. 1994, 233, 250.
48. Hevel, J. M.; White, K. A. J. Biol. Chem. 1991, 266, 22789.
49. Wolfenden, B. S.; Willson, R. L. J. Chem. Soc. Perkin Trans. 1982, 2, 805 1982.
50. Rice-Evans, C. A.; Miller, N. J.; Bolwell, G. P.; Bramley, P. M.; Pridham, J. B. Free Radic. Res. 1995, 22, 375.
51. Miller, N. J.; Sampson, J.; Candeias, L. P.; Bramley, P. M.; Rice-Evans, C. A. Antioxidant activities of carotenes and xanthophylls. FEBS Lett. 1996, 384, 240.
52. Cotelle, A,; Bernier, J.L.; Catteau, J.P.; Pommery, J.; Wallet, J.C.; Gaydou, E.M. Free Radic Biol Med, 1996, 20, 35.
53. Brand-Williams, W.; Cuvelier, M.E.; Berset, C.; Leben.-Wiss, W. Technol. Food Sci. Technol. 1995, 28, 25.
54. Organic chemistry portal. Osiris Property Explorer. Retrieved 3 March 2011, from http://www.organic-chemistry.org/prog/peo/